



## A discoloration study of a series of cationic organic dyes in acidic and alkaline pH using Mn ferrite nanocatalyst

Payman Roonasi

Department of Chemistry, Kharazmi University, Karaj, P.O. Box 15719-14911, Tehran, Iran, email: payman\_roonasi@yahoo.com

Received 12 February 2017; Accepted 27 August 2017

### ABSTRACT

The aim of this study was to synthesize manganese ferrite nanoparticles with strong magnetic and catalytic properties for effective discoloration of organic dyes in wastewater. The catalyst synthesis was carried out by coprecipitation method and characterized using different techniques. The synthetic Mn ferrite showed characteristic of spinel type structure and small nanometer-sized particles. It was found that the catalyst is capable of discoloration of three cationic dyes in acidic and alkaline conditions. At low pH, low catalyst loading and low  $H_2O_2$  concentration were sufficient to achieve complete discoloration of the dyes. At high pH, however, increasing  $H_2O_2$  concentration and catalyst loading both increases discoloration of the dyes. In a comparison between acidic and alkaline condition, it was concluded that the catalyst is more efficient in acidic medium. Under alkaline condition, the dye should be basically adsorbed at the catalyst surface in order to effectively react with  $H_2O_2$  and to be consequently decomposed. This study particularly highlights the importance of surface in reaction of hydrogen peroxide with cationic dyes being adsorbed under alkaline condition.

*Keywords:* Manganese ferrite; Heterogeneous Fenton-like catalyst; Cationic organic dye; Discoloration; Magnetic nanoparticle; Surface properties

### 1. Introduction

Fenton and Fenton-like reactions are advanced oxidation technologies used for oxidation and degrading a large variety of organic toxic compounds into harmless materials (e.g.,  $CO_2$  and  $H_2O$ ).

In classic Fenton reaction, hydrogen peroxide and  $Fe^{2+}$  ions are often used to produce  $\cdot OH$  radical, a very strong oxidizing agent. Since several drawbacks have been pointed out in literature for classic Fenton process, heterogeneous Fenton-like catalysis has recently gained great attention [1–5]. Some examples of heterogeneous catalysts applied in Fenton-like reactions are clays, iron oxide minerals, resin-supported  $Fe^{2+}$  or  $Fe^{3+}$ , zeolites exchanged with iron or copper ions, and synthetic nanoparticles, the majority of them contain iron compounds.

Ferrites are iron(III) oxide based ceramic materials. The main type of ferrites is spinel type with the formula  $MFe_2O_4$  and a cubic crystal structure in which oxygen ions form a cubic closed-pack motif and the cations occupy tetrahedral and octahedral holes. Due to their structural, electronic,

magnetic and catalytic properties, as well as chemical stability, and low cost, they have been broadly used for many different technological applications. There are also several studies on utilization of different ferrites for wastewater treatment [6–10].

The high magnetic properties of these materials can be used for magnetic separation and recovery of the catalysts. The small size and a large number of reactive surface sites make ferrite nanoparticle an appropriate catalyst/adsorbent for contaminants including dyes.

Manganese ferrite is one of the ferrite with strong magnetic property and high catalytic active which has been used for removal of organic dyes. Wu and Qu [11] synthesized  $MnFe_2O_4$  and used it as adsorbent of water-soluble azo dyes. After adsorption of dyes on the Mn ferrite surface, the Mn ferrite surface was regenerated in a separate step, by using Fenton's reagents (i.e.,  $Fe^{2+}$  and  $H_2O_2$ ) for oxidation and degradation of the dyes. In another study, Wu et al. [12] regenerated their Mn ferrite adsorbent by thermal degradation in a muffle furnace and washing it with NaOH solution. Wang et al. [13] synthesized metal ferrite (Mn, Co, Ni and Fe)

magnetic nanoparticles as adsorbent for Congo red dye. The nanocrystalline ferrites showed strong magnetic property and high adsorption capacity for this dye. For regeneration of ferrite, acetone or alcohol was used for desorption of the adsorbed dye. In addition,  $Mn_xFe_{3-x}O_4$  was synthesized through solvothermal route to be utilized as heterogeneous Fenton-like catalyst [14]. In this synthetic method, the iron and manganese salts were dissolved in ethylene glycol and heated to 200°C for 8 h. However, they did not measure the amount of dye adsorption on the catalyst surface, the catalyst showed high catalytic reactivity as well as good recyclability. They observed that, the degradation reaction of methylene blue can be completed within about 6 h at neutral pH, using this catalyst.

In addition to the abovementioned properties of Mn ferrite reported from the literature, this work presents a highly active manganese ferrite, synthesized via a simple method for one step discoloration and a fast reaction rate which works in different pH range.

Therefore, the central aim of this work was to study surface properties of magnetic nanoparticles of the type Mn ferrite as Fenton-like catalyst and to examine the optimum working condition for degradation of cationic dyes, as model contaminants, at acidic and alkaline condition. Hydrogen peroxide, which has been used as oxidizing agent in wastewater treatment for years, was also applied together with the catalyst. The oxidation rates of a number of cationic dyes were followed by measuring absorbance at characteristic band of the examined dye in UV–Vis spectrophotometer. The measurements were carried out in acidic and alkaline media and in each case, the proper condition was investigated.

## 2. Materials and methods

### 2.1. Reagents

Manganese(II) chloride tetrahydrate, iron(III) chloride hexahydrate, sodium hydroxide and hydrogen peroxide solution (30% w/w in water) were purchased from Merck (Darmstadt, Germany). Distilled water was used in all synthesis and rinsing processes and also decomposition reactions.

### 2.2. Organic dyes

The commercial organic dyes used in this work were methylene blue ( $\lambda_{\max} = 664$  nm), basic yellow 28 ( $\lambda_{\max} = 440$  nm) and basic violet 16 ( $\lambda_{\max} = 545$  nm).

### 2.3. Catalyst synthesis

A mixture of manganese(II) chloride and iron(III) chloride with 1:2 molar ratio and total metal concentration of 0.3 M were initially dissolved in 100 mL distilled water. The mixed salt solution was then added dropwise into a 100 mL vigorously stirred 3 M NaOH solution preheated to 95°C. After the addition was completed, the reaction mixture was aged at this temperature for another 2 h to get a powder precipitate. The precipitate was separated by decantation and washed with distilled water. The last step was repeated for several times. The solid residue was eventually centrifuged and dried at 70°C for 10 h.

### 2.4. Characterization of the synthetic catalyst nanoparticles

The sample was characterized by infrared spectroscopy (IR), X-ray powder diffraction (XRD) and scanning electron microscopy (SEM). The infrared spectrum of the ferrite sample was collected in the range of 400–4,000  $\text{cm}^{-1}$  on a PerkinElmer RXI FTIR instrument. The X-ray diffractogram of the powder sample was recorded on a X'Pert Pro MPD diffractometer in  $2\theta$  range 20–700 with Cu  $K\alpha$  radiation ( $\lambda = 1.54056$  Å). SEM was run on a Philips XL 30. The magnetic property of the sample was measured using a vibrating sample magnetometer (VSM; BHV-55, Riken, Japan) at room temperature.

### 2.5. Dye concentration measurement

Concentrations of the dyes were measured on a Cintra 101 GBS UV–Vis spectrophotometer. A pair of cells (cuvettes) made of quartz and with a thickness of 1 cm was used. A calibration curve was drawn for each dye at its maximum absorption wavelength ( $\lambda_{\max}$ ) vs. concentration. Each of the removal experiment in the following sections was conducted using single dye at a time to avoid possible overlapping of the absorption spectra of the dyes.

### 2.6. Removal rate of dyes by the ferrite catalyst

Removal rate is expressed here as the ratio  $(C_0 - C)/C_0$  (where  $C_0$  is the initial dye concentration and  $C$  is the concentration at any time  $t$ ) with time. Removal rate of the dyes in the presence of the catalyst and  $H_2O_2$  was monitored by measuring absorbance at  $\lambda_{\max}$  of the dye under investigation in UV–Vis spectrophotometer. In each case,  $(C_0 - C)/C_0 \times 100$  was plotted against time. All reactions were carried out at room temperature and in dark with the initial dye concentration of 50 ppm. Whenever needed, HCl and/or NaOH were used to adjust the pH. Every time, the reaction was initiated by adding a given amount of concentrated hydrogen peroxide solution (30%) to the mixture of the catalyst and the dye solution ( $t = 0$ ). The suspension containing the catalyst and the solution in a fully covered with aluminum foil stoppered flask, was stirred using a magnetic stirrer bar, while at given intervals, the samples were taken, centrifuged, and absorbance of the supernatant was immediately measured.

### 2.7. Dye adsorption measurement

Adsorption of dyes at the catalyst surface was measured by adding the dye solution with initial concentration of 50 ppm and at pH 10 to 2, 5 and 10 g/L catalyst. No hydrogen peroxide or inert electrolyte was added to the solution for adsorption measurement.

### 2.8. Evaluation of $H_2O_2$ concentration and catalyst loading effect

Similar procedure as above was applied for evaluation of the effect of hydrogen peroxide and catalyst loading on discoloration of the dyes, except that, in this case NaCl was added to desorb the electrostatically adsorbed dye from the surface back into the solution. At constant 2 g/L catalyst, hydrogen peroxide concentration varied between 0.015, 0.1 and 0.5 M. Also, with constant  $H_2O_2$  concentration of 0.5 M,

the catalyst loading was set at 2, 5 and 10 g/L. At the end of each reaction and before reading the absorbance, NaCl was added.

### 2.9. Reusability of the catalyst

The reusability of the catalyst was tested by filtration of the suspension of catalyst and dyes solution at the end of the discoloration reaction, and after separation of the supernatant, the recovered catalyst was redispersed in a new batch of fresh solution of dye and  $H_2O_2$  for a new run. This procedure was repeated four times.

## 3. Results and discussion

### 3.1. Catalyst characterization

The structural properties of the synthetic catalyst were obtained by XRD, FTIR, SEM and VSM techniques and are illustrated in Figs. 1(a)–(d), respectively. The XRD pattern shows characteristic peaks of spinel phase crystallites where the peaks from left to right are assigned to 220, 311, 400, 422, 511 and 440 reflections (PDF #10-0319). The peak broadening is due to the small crystallite size of the catalyst. The SEM image of the sample catalyst also demonstrates aggregated nanometer-sized particles. In infrared spectrum, the broad bands below  $1,000\text{ cm}^{-1}$  are assigned to metal oxygen bond vibration, while, the broad and strong features above  $3,000\text{ cm}^{-1}$  and the bands around  $1,600\text{--}1,300\text{ cm}^{-1}$  are, respectively, assigned to stretching and bending vibrations of OH bonded metal. This surface OH group is believed to be an indication of the catalyst active sites [15,16].

The synthetic Mn ferrite also strongly responded to a magnetic field and VSM measurement showed super paramagnetic behavior of the particles with a saturation magnetization (Ms) of  $58.2\text{ emu/g}$ , in agreement with its spinel structure and good magnetic property [14,17].

### 3.2. Catalytic activity of the catalyst

An overview of the literature on catalytic activity of different catalysts generally shows that most catalysts are more efficient in acidic condition. This study not only compares the catalytic activity of the synthetic Mn ferrite under acidic and alkaline condition, but also it deals with how some parameters affect the efficiency of the catalyst under alkaline condition in order to optimize the reaction condition for discoloration of cationic dyes.

#### 3.2.1. Alkaline condition

**3.2.1.1. Adsorption of the dyes at the catalyst surface** Adsorption of the three studied cationic dyes at the catalyst surface at pH 10 is depicted in Fig. 2. It has been found that the point of zero charge of Mn ferrite is  $<5$  [11,13]. This indicates that the Mn ferrite surface is negatively charged at pH 10. On the other hand, the pKa value of methylene blue is 3.8 and above this pH, the molecule is positively charged. Similarly, basic violet dissociates to a cationic dye and  $Cl^-$  and has pKa values of  $pK_{a1} = 5.31$ ;  $pK_{a2} = 8.64$  at pH 10 where the positive charges are localized on nitrogen atoms and basic yellow 28 dissociates to  $CH_3SO_4^-$  and the positively charged cationic dye [18].

Therefore, it turns out that at pH 10, the catalyst surface is negatively charged and could readily adsorb positively charged cationic dyes. It was noticed that adding high concentration NaCl led to almost complete desorption, returning the concentration in solution to nearly its original (more than 90% of the initial dye concentration was reached) for all three studied dyes. This indicates that the adsorption is electrostatic physical adsorption rather than chemisorption. It is known that strong electrolytes such as NaCl or NaOH may affect adsorption of ionic dyes, albeit depending on the nature of interaction, that is, when interaction between

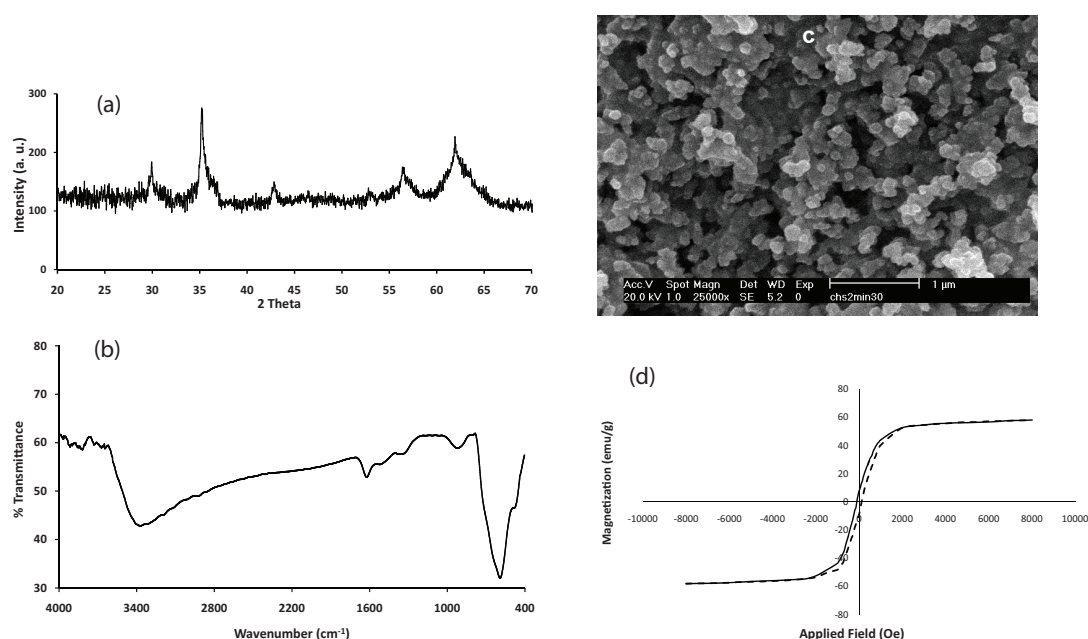


Fig. 1. (a) XRD pattern, (b) IR spectrum, (c) SEM image and (d) VSM of the Mn ferrite sample.

the dye and catalyst is electrostatic. The presence of these electrolytes in solution may compete for active sites on the catalyst surface and replace electrostatically adsorbed cationic or anionic dyes [19–21]. Furthermore, according to the electrical double layer theory, an increase in ionic strength results in a compression of electrical double layer, leading to a reduction of surface potential [22,23]. The consequence is a decrease in electrostatic adsorption capacity of the catalyst. Moreover, adsorption of the dyes increases with raising catalyst loading, so that, depending on the dye, about 40%–90% of the dyes were adsorbed when, respectively, 2–10 g/L catalyst were used. Increasing adsorption is the result of having higher surface area and hence, more surface sites are available for adsorption of dyes with more catalyst addition.

**3.2.1.2. Discoloration of the dyes with the catalyst** In this study, discoloration is considered to be the fall in concentration of the dye molecule in solution, which may be the result of oxidation or breaking down of the dye molecule into smaller products. Such definition excludes surface physical adsorption; however, it does not imply that the oxidation reaction necessarily goes to complete decomposition of the molecules to the end products ( $\text{CO}_2$  and  $\text{H}_2\text{O}$ ). As a matter of fact, a number of colorless intermediates along with detailed mechanisms have been found and proposed for degradation of methylene blue, basic violet and basic yellow in the literature [24–26]. Besides, several studies have shown decomposition of  $\text{H}_2\text{O}_2$  to hydroxyl radical and other active species in the presence of Mn ferrite nanoparticles [17,27,28]. Bearing this in mind, discoloration was studied by measuring concentration of the dye after treating it with different concentrations of hydrogen peroxide and the catalyst under alkaline condition. Each time after the  $\text{H}_2\text{O}_2$  treatment, high concentration NaCl was added to remove electrostatically adsorbed dye from the catalyst surface. In this way, any non-degraded dye molecule that remained adsorbed at the surface, is replaced by  $\text{Na}^+$  ions, and dissolve back into the solution to be detected. In the next part, the effects of hydrogen peroxide concentration and catalyst loading on degradation of the dyes were examined in order

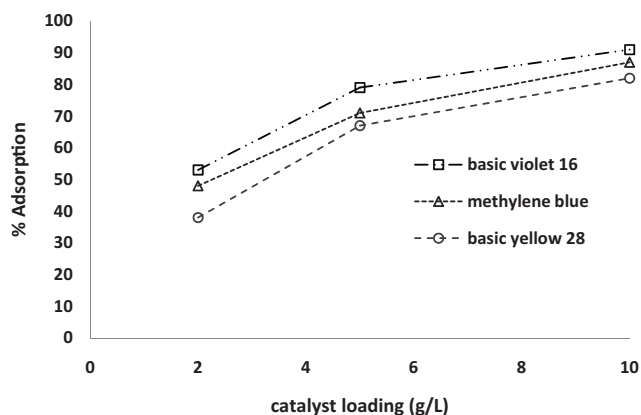


Fig. 2. Adsorption of dyes on catalyst surface at pH 10. Initial dye concentration = 50 ppm, catalyst loadings = 2, 5 and 10 g/L as illustrated in the figure.

to find the optimum hydrogen peroxide concentration and catalyst loading for discoloration of the dyes under alkaline condition.

**3.2.1.3. Effect of  $\text{H}_2\text{O}_2$  concentration and catalyst loading on the dyes discoloration** Fig. 3 shows the effect of  $\text{H}_2\text{O}_2$  concentration and catalyst loading on discoloration of the dyes. As seen, raising  $\text{H}_2\text{O}_2$  concentration and catalyst loading both increases discoloration of the dyes. Taking methylene blue as an example, 33% more oxidation took place when  $\text{H}_2\text{O}_2$  concentration goes up from 0.015 to 0.5 M, at 2 g/L catalyst loading. Likewise, discoloration is 40% higher with raising catalyst loading from 2 to 10 g/L (at 0.5 M  $\text{H}_2\text{O}_2$ ). This effect follows the same trend for the other two dyes. This may be explained by taking into account that at higher catalyst loading, adsorption of both reactants, that is,  $\text{H}_2\text{O}_2$  and the dye are larger. Having more reactants in close contact, the reaction rate is higher. This matter is discussed later in this section. Here, note the difference between Figs. 2 and 3. Fig. 2 shows only adsorption of the dyes, while Fig. 3 demonstrates the amount of dyes degradation. As mentioned in section 3.2.1.2 for degradation study (Fig. 3) NaCl was added to remove adsorbed dye molecules, however, in the case of adsorption (Fig. 2), no NaCl was added (see sections 2.7 and 2.8).

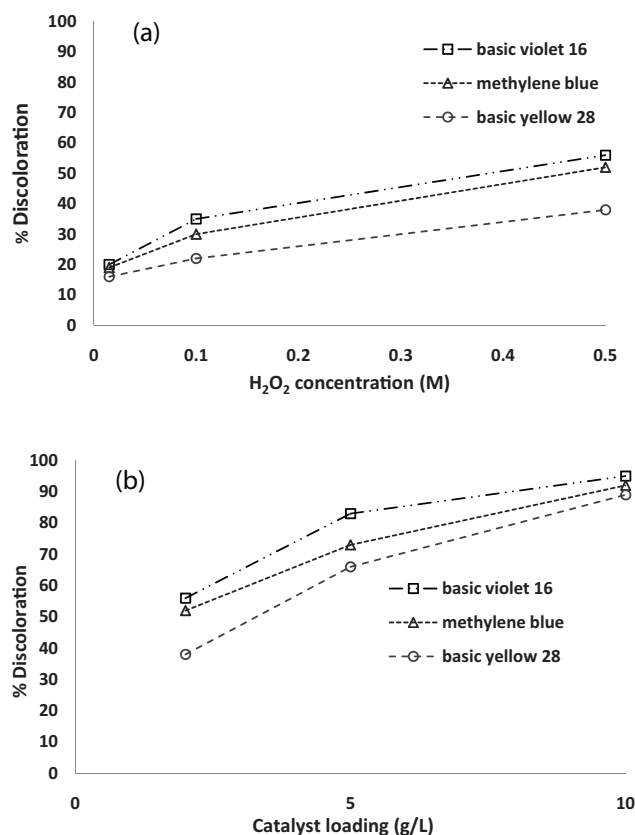


Fig. 3. Effect of (a)  $\text{H}_2\text{O}_2$  concentration and (b) catalyst loading on discoloration of the dyes. Initial dyes concentrations  $C_{\text{dye}} = 50$  ppm, in (a) 2 g/L catalyst and in (b) 0.5 M  $\text{H}_2\text{O}_2$  were used.



**3.2.1.4. Removal rate of the dyes** Fig. 4(a) illustrates the plot of dye removal (in percentage) vs. time for the three studied dyes at pH = 10, when 2 g/L catalyst and 15 mM  $H_2O_2$  concentration was employed. There is a relatively great increase in dyes removal in the beginning of the reaction which is partly related to physical adsorption of the dyes at the surface and partly because of decomposition of the dyes by hydrogen peroxide. As noted earlier, positively charged cationic dyes adsorb on negatively charged particles surface at alkaline condition of pH 10. Also, hydrogen peroxide in alkaline condition decomposes to produce different active species such as  $\cdot OH$ ,  $\cdot OOH$  and high-valent iron species ( $Fe^{IV}=O$  and  $Fe^V=O$ ) which can oxidize organic dyes. Adding NaCl to the solution at the end of the reaction time, results in partial desorption (17%, 24% and 10%, respectively, for methylene blue, basic violet and basic yellow) of the dye from the catalyst surface (compare the points at 240 min in Fig. 4(a) with the corresponding's in Fig. 3(a) at 2 g/L catalyst loading and 0.015 M  $H_2O_2$ ), attesting that under these operating circumstances electrostatic physical adsorption takes place in parallel with decomposition reaction.

Fig. 4(b) shows a sharp rise in removal of the dyes at the very early stage of reactions for the case of 10 g/L catalyst loading and 0.5 M  $H_2O_2$  concentration. As described in experimental section, each dye at pH 10, first is mixed and adsorbed at the catalyst surface prior to  $H_2O_2$  addition.

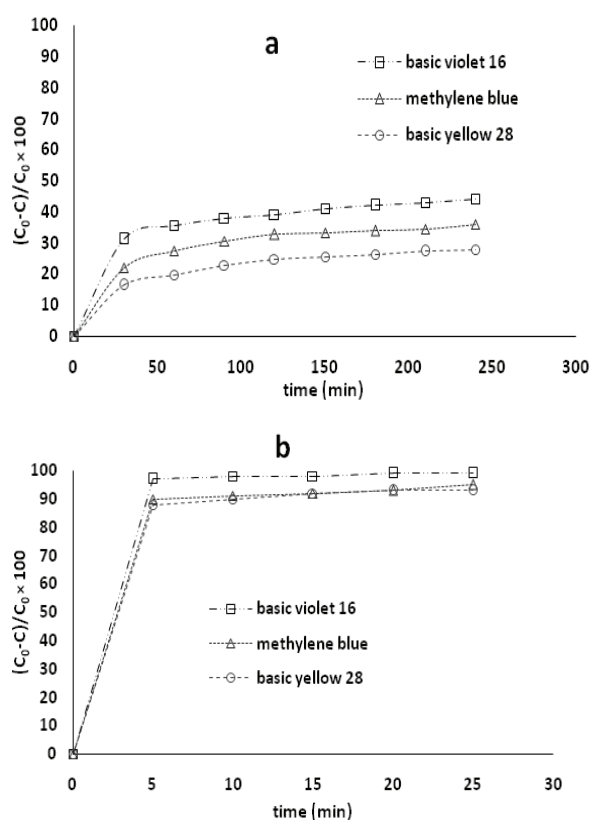


Fig. 4. Removal rate of methylene blue, basic yellow and basic violet with (a)  $C_{H_2O_2} = 15$  mM and 2 g/L catalyst, and (b)  $C_{H_2O_2} = 0.5$  M and 10 g/L catalyst. Initial dyes concentrations  $C_{dye} = 50$  ppm and pH = 10.

A severe discoloration of the solution is seen even at this stage, probably owing to the rapid and substantial physical adsorption. By addition of  $H_2O_2$ , the already adsorbed dye molecules at the surface reacts with the active species ( $\cdot OH$ ,  $\cdot OOH$ , etc.) produced from  $H_2O_2$  at the surface. The consequence of this reaction is degradation of dye. No significant desorption occurred by adding NaCl to the mixture of dye and catalyst treated with  $H_2O_2$ , implying that the dye is almost totally oxidized (to colorless intermediate or final oxidation products) at the surface.

It is well-known that unlike the acidic medium where  $H_2O_2$  is more stable, hydrogen peroxide may quickly decompose into  $H_2O$  and  $O_2$  under alkaline condition. Indeed, the reaction passes through intermediate active species. Since  $H_2O_2$  decomposition occurs on the periphery of the catalyst surface, it is more plausible to interact with adsorbed dye molecules (also close to the surface) than those in the solution. If the intermediate active species do not meet and interact with adsorbed dye molecules, they may interact directly with each other to form  $H_2O$  and  $O_2$ .

### 3.2.2. Acidic condition

Fig. 5 demonstrates a plot of dye discoloration (in percentage) vs. time for the three studied dyes at pH = 3.5. As it can be seen in this figure, in the presence of only 15 mM hydrogen peroxide and 2 g/L catalyst, complete discolorization was observed for all three cationic dyes within 4 h. The variation in degradation rates of the different dyes might be related to the different activation energy of oxidation of each dye.

It is obvious that, adsorption of cationic dyes on catalyst surface is low at this pH (<5%). It should be noted that the reaction rate is negligible when the Mn ferrite catalyst is excluded from the reaction mixture. Thus, the presence of  $H_2O_2$  together with the catalyst is basically necessary in order to increase the reaction rate. Generally, the heterogeneous catalysis in Fenton reaction, the surface Fe and/or other transition metals cations possess unoccupied d-orbitals with which oxygen atoms of the initially adsorbed hydrogen peroxide may react. Depending on the operating condition such as the solution pH, it may result in different active species. In acidic condition,  $\cdot OH$  radical is generated by following the reaction of hydrogen peroxide with the catalyst. In fact,  $\cdot OH$

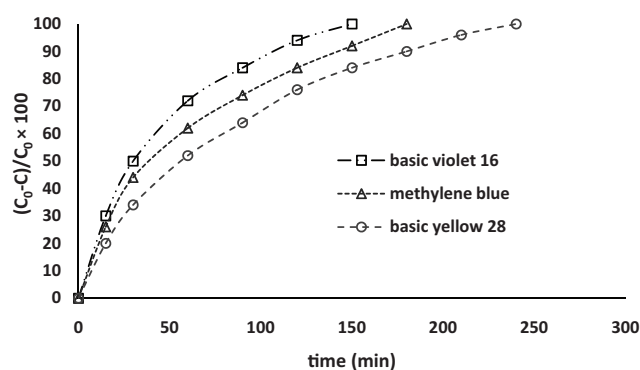
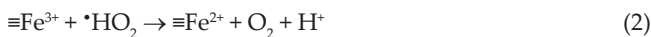
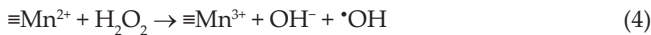


Fig. 5. Removal rate of methylene blue, basic yellow and basic violet in acidic medium. The reaction conditions were: pH 3.5, initial dyes concentrations 50 ppm, 2 g/L catalyst and  $C_{H_2O_2} = 15$  mM.

is a very active oxidizing agent which can attack a wide range of organic compounds. Different mechanisms have been suggested for the  $\cdot\text{OH}$  formation, probably the most accepted one is based on redox action of the  $\text{Fe}^{2+}/\text{Fe}^{3+}$  as described by the following equations [29–31]:



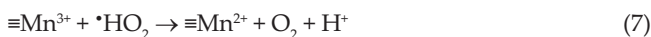
It has been shown that Mn in spinel structure has remarkable effect on the activity of the ferrite catalyst promoting hydrogen peroxide decomposition rate and also oxidation of organic contaminants [32–34]. Thus, in addition to  $\text{Fe}^{2+}/\text{Fe}^{3+}$  reaction,  $\text{Mn}^{2+}/\text{Mn}^{3+}$  may also undergo redox reactions to facilitate  $\cdot\text{OH}$  production as follows:



The surface  $\text{Mn}^{3+}$  then may be reduced back to  $\text{Mn}^{2+}$  by the following reaction:



where Fe ions may be the surface Fe or bulk Fe ions. An alternative mechanism for transformation of  $\text{Mn}^{3+}$  back to  $\text{Mn}^{2+}$  might be the reaction of  $\text{Mn}^{3+}$  with  $\text{H}_2\text{O}_2$ , similar to Eqs. (1) and (2).



Another possible mechanism is decomposition of  $\text{H}_2\text{O}_2$  into  $\cdot\text{OH}$  radicals through direct O–O bond cleavage [31]. The formed OH radical then can readily react with the organic dye and decompose it. To assess whether the dye is adsorbed or decomposed at the surface, NaCl was added to the mixture at the end of the reaction. No desorption was observed by adding NaCl to the solution at this stage, indicating that the dye has been essentially decomposed (to colorless intermediate or final oxidation products) by hydrogen peroxide at the catalyst surface.

### 3.3. Reusability of the catalyst

The reusability of the catalyst was investigated in acidic and alkaline conditions and the results are shown in Figs. 6(a) and (b), respectively. In acidic condition, the catalyst retained its activity after four time use. On the other hand, the efficiency of the catalyst rather diminished every time under alkaline condition. Numerically, the catalyst activity dropped to 78% in the fourth run. This is probably due to incomplete or partial decomposition of the dye into intermediate organic molecules that remain adsorbed on the catalyst surface. These molecules occupy active sites of the

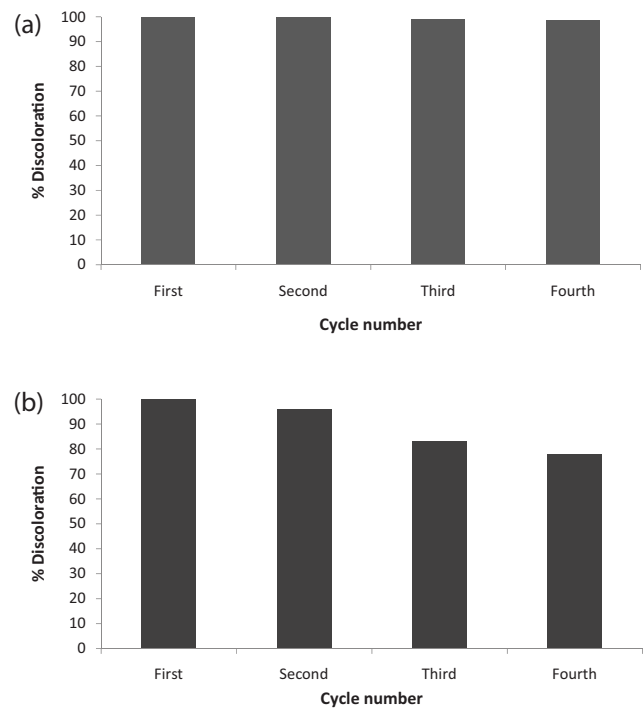


Fig. 6. Reusability of the catalyst for discoloration of methylene blue with initial dye concentration of 50 ppm; (a) pH = 3.5, 2 g/L catalyst,  $C_{\text{H}_2\text{O}_2} = 15$  mM; and (b) pH = 10, 10 g/L catalyst,  $C_{\text{H}_2\text{O}_2} = 0.5$  M.

catalyst which could bring about poisoning and reducing its catalytic activity. Actually, it was found that adsorption of the dye on catalyst surface decreases in consecutive runs, which may explain the lower activity of the catalyst in the next runs.

### 3.4. Comparison between acidic and alkaline conditions

As shown above, both acidic and alkaline conditions could be used for effective discoloration of the dyes, however, with different operational settings. The advantage of acidic medium is low catalyst and low concentration needed for full discoloration of the dyes and its better reusability. Even more important is that anionic dye can be degraded under acidic condition. Nonetheless, metal leaching is more likely to occur in low pH values and it takes longer time to complete the reaction. On the other hand, the reaction rate was found to be very high under alkaline condition. Despite the high reaction rate, alkaline condition is in general less effective and reusable than acidic condition. In real system, where there are mixed anionic and cationic dyes in industrial effluents, acidic condition seems to be more efficient.

## 4. Conclusion

Discoloration of organic dyes with synthetic Mn ferrite in low and high pH values was studied. It was found that synthetic Mn ferrite could be effectively used for discoloration of the three cationic organic dyes in both acidic and alkaline conditions under different operational settings. At low pH, low catalyst loading and low  $\text{H}_2\text{O}_2$  concentration was sufficient for total discoloration of the dyes. The mechanism

probably includes  $\text{Fe}^{2+}/\text{Fe}^{3+}$  and  $\text{Mn}^{2+}/\text{Mn}^{3+}$  redox reactions, leading to active radical formation. The active radical may then react with the organic dye; the consequence of this reaction is decomposition and degradation of the organic dyes. To differentiate between physical adsorption and degradation, NaCl as an inert electrolyte was employed. No desorption was observed by adding NaCl to the treated mixture of dye and catalyst with  $\text{H}_2\text{O}_2$  at low pH.

At high pH, high concentration of catalyst was needed for adequate adsorption of the organic dyes at the catalyst surface to efficiently react with hydrogen peroxide. Fast decomposition of  $\text{H}_2\text{O}_2$  into active species at high pH which may react with the dye molecules on the periphery of the catalyst seems to be responsible for discoloration of the organic dyes under alkaline condition. It can be concluded that the influence of surface is essential in all cases on discoloration of organic dyes using Mn ferrite catalyst.

### Acknowledgment

The author would like to thank Kharazmi University for providing financial support.

### References

- [1] E.G. Garrido-Ramírez, B.K.G. Theng, M.L. Mora, Clays and oxide minerals as catalysts and nanocatalysts in Fenton-like reactions – a review, *Appl. Clay Sci.*, 47 (2010) 182–192.
- [2] A. Georgi, A. Schierz, U. Trommler, C.P. Horwitz, T.J. Collins, F.D. Kopinke, Humic acid modified Fenton reagent for enhancement of the working pH range, *Appl. Catal., B*, 72 (2007) 26–36.
- [3] M.M. Cheng, W.H. Ma, J. Li, Y.P. Huang, J.C. Zhao, Visible light-assisted degradation of dye pollutants over Fe(III)-loaded resin in the presence of  $\text{H}_2\text{O}_2$  at neutral pH values, *Environ. Sci. Technol.*, 38 (2004) 1569–1575.
- [4] K. Hanna, T. Kone, G. Medjahdi, Synthesis of the mixed oxides of iron and quartz and their catalytic activities for the Fenton-like oxidation, *Catal. Commun.*, 9 (2008) 955–959.
- [5] C. Catrinescu, M. Teodosiu, M. Macoveanu, J. Míche-Brendlé, R. Le Dred, Catalytic wet peroxide oxidation of phenol over Fe-exchanged pillared beidellite, *Water Res.*, 37 (2003) 1154–1160.
- [6] L. Shao, Z. Ren, G. Zhang, L. Chen, Facile synthesis, characterization of a  $\text{MnFe}_2\text{O}_4$ /activated carbon magnetic composite and its effectiveness in tetracycline removal, *Mater. Chem. Phys.*, 135 (2012) 16–24.
- [7] A.A. Farghali, M. Moussa, M.H. Khedr, Synthesis and characterization of novel conductive and magnetic nanocomposites, *J. Alloys Compd.*, 499 (2010) 98–103.
- [8] J. Zhang, J. Zhuang, L. Gao, Y. Zhang, N. Gu, J. Feng, D. Yang, J. Zhu, X. Yan, Decomposing phenol by the hidden talent of ferromagnetic nanoparticles, *Chemosphere*, 73 (2008) 1524–1528.
- [9] M.A. Valenzuela, P. Bosch, J. Jimenez-Becerrill, O. Quiroz, A.I. Paez, Preparation, characterization and photocatalytic activity of  $\text{ZnO}$ ,  $\text{Fe}_2\text{O}_3$  and  $\text{ZnFe}_2\text{O}_4$ , *J. Photochem. Photobiol., A*, 148 (2002) 177–182.
- [10] E. Casbeer, V.K. Sharma, X.-Z. Li, Synthesis and photocatalytic activity of ferrites under visible light: a review, *Sep. Purif. Technol.*, 87 (2012) 1–14.
- [11] R. Wu, J. Qu, Removal of water-soluble azo dye by the magnetic material  $\text{MnFe}_2\text{O}_4$ , *J. Chem. Technol. Biotechnol.*, 80 (2005) 20–27.
- [12] R. Wu, J. Qu, Y. Chen, Magnetic powder  $\text{MnO-Fe}_2\text{O}_3$  composite—a novel material for the removal of azo-dye from water, *Water Res.*, 39 (2005) 630–638.
- [13] L. Wang, J. Li, Y. Wang, L. Zhao, Q. Jiang, Adsorption capability for Congo red on nanocrystalline  $\text{MFe}_2\text{O}_4$  ( $M = \text{Mn, Fe, Co, Ni}$ ) spinel ferrites, *Chem. Eng. J.*, 181–182 (2012) 72–79.
- [14] M. Li, Q. Gao, T. Wang, Y.S. Gong, B. Han, K.S. Xia, C.G. Zhou, Solvothermal synthesis of  $\text{Mn}_x\text{Fe}_{3-x}\text{O}_4$  nanoparticles with interesting physicochemical characteristics and good catalytic degradation activity, *Mater. Des.*, 97 (2016) 341–348.
- [15] S. Xing, C. Hu, J. Qu, H. He, M. Yang, Characterization and reactivity of  $\text{MnO}_x$  supported on mesoporous zirconia for herbicide 2,4-D mineralization with ozone, *Environ. Sci. Technol.*, 42 (2008) 3363–3368.
- [16] T. Zhang, C. Li, J. Ma, H. Tian, Z. Qiang, Surface hydroxyl groups of synthetic  $\alpha\text{-FeOOH}$  in promoting  $\cdot\text{OH}$  generation from aqueous ozone: property and activity relationship, *Appl. Catal., B*, 82 (2008) 131–137.
- [17] U.S. Sharma, R.N. Sharma, R. Shah, Physical and magnetic properties of manganese ferrite nanoparticles, *Int. J. Eng. Res. Appl.*, 4 (2014) 14–17.
- [18] W. Konicki, K. Cendrowski, G. Bazarko, E. Mijowska, Study on efficient removal of anionic, cationic and nonionic dyes from aqueous solutions by means of mesoporous carbon nanospheres with empty cavity, *Chem. Eng. Res. Des.*, 94 (2015) 242–253.
- [19] N.M. Mahmoodi, B. Hayati, M. Arami, Textile dye removal from single and ternary systems using date stones: kinetic, isotherm, and thermodynamic studies, *J. Chem. Eng. Data*, 55 (2010) 4638–4649.
- [20] A.M. Donia, A.A. Atia, W.A. Al-amrani, A.M. El-Nahas, Effect of structural properties of acid dyes on their adsorption behaviour from aqueous solutions by amine modified silica, *J. Hazard. Mater.*, 161 (2009) 1544–1550.
- [21] T. Xing, H. Kai, G. Chen, Study of adsorption and desorption performance of acid dyes on anion exchange membrane, *Color. Technol.*, 128 (2012) 295–299.
- [22] P. Punjongharn, K. Meevasana, P. Pavasant, Influence of particle size and salinity on adsorption of basic dyes by agricultural waste: dried Seagrass (*Caulerpa lentillifera*), *J. Environ. Sci.*, 20 (2008) 760–768.
- [23] D.J. Shaw, Introduction to Colloid and Surface Chemistry, Chapter 7, 4th ed., Butterworth-Heinemann, Oxford, 1992.
- [24] Q. Wang, S. Tian, P. Ning, Degradation mechanism of methylene blue in a heterogeneous Fenton-like reaction catalyzed by ferrocene, *Ind. Eng. Chem. Res.*, 53 (2014) 643–649.
- [25] W.H. Chung, C.S. Lu, W.Y. Lin, J.X. Wang, C.W. Wu, C.C. Chen, Determining the degradation efficiency and mechanisms of ethyl violet using HPLC-PDA-ESI-MS and GC-MS, *Chem. Cent. J.*, 6 (2012) 63–75.
- [26] M. Iranifam, M. Zarei, A.R. Khataee, Decolorization of C.I. Basic Yellow 28 solution using supported  $\text{ZnO}$  nanoparticles coupled with photoelectro-Fenton process, *J. Electroanal. Chem.*, 659 (2011) 107–112.
- [27] P. Baldrian, V. Merhautova, J. Gabriel, F. Nerud, P. Stopka, M. Hruby, M.J. Benes, Decolorization of synthetic dyes by hydrogen peroxide with heterogeneous catalysis by mixed iron oxides, *Appl. Catal., B*, 66 (2006) 258–264.
- [28] T. Valdes-Solis, P. Valle-Vigon, S. Alvarez, G. Marban, A.B. Fuertes, Manganese ferrite nanoparticles synthesized through a nanocasting route as a highly active Fenton catalyst, *Catal. Commun.*, 8 (2007) 2037–2042.
- [29] W.P. Kwan, B.M. Voelker, Rates of hydroxyl radical generation and organic compound oxidation in mineral-catalyzed Fenton-like systems, *Environ. Sci. Technol.*, 37 (2003) 1150–1158.
- [30] W. Luo, L. Zhu, N. Wang, H. Tang, M. Cao, Y. She, Efficient removal of organic pollutants with magnetic nanoscaled  $\text{BiFeO}_3$  as a reusable heterogeneous Fenton-like catalyst, *Environ. Sci. Technol.*, 44 (2010) 1786–1791.
- [31] J. Yan, H. Tang, Z. Lin, M. Naveed Anjum, L. Zhu, Efficient degradation of organic pollutants with ferrous hydroxide colloids as heterogeneous Fenton-like activator of hydrogen peroxide, *Chemosphere*, 87 (2012) 111–117.
- [32] R.C.C. Costa, M.F.F. Lelis, L.C.A. Oliveira, J.D. Fabris, J.D. Ardisson, R.R.V.A. Rios, C.N. Silva, R.M. Lago, Remarkable effect of Co and Mn on the activity of  $\text{Fe}_{3-x}\text{M}_x\text{O}_4$  promoted oxidation of organic contaminants in aqueous medium with  $\text{H}_2\text{O}_2$ , *Catal. Commun.*, 4 (2003) 525–529.

- [33] R.C.C. Costa, M.F.F. Lelis, L.C.A. Oliveira, J.D. Fabris, J.D. Ardisson, R.R.V.A. Rios, C.N. Silva, R.M. Lago, Novel active heterogeneous Fenton system based on  $\text{Fe}_{3-x}\text{M}_x\text{O}_4$  (Fe, Co, Mn, Ni): the role of  $\text{M}^{2+}$  species on the reactivity towards  $\text{H}_2\text{O}_2$  reactions, *J. Hazard. Mater.*, B129 (2006) 171–178.
- [34] P. Lahiri, S.K. Sengupta, Physico-chemical properties and catalytic activities of the spinel series  $\text{Mn}_x\text{Fe}_{3-x}\text{O}_4$  towards peroxide decomposition, *J. Chem. Soc., Faraday Trans.*, 91 (1995) 3489–3494.